ACS Catalysis

Research Article

Cite This: ACS Catal. 2018, 8, 596–601

pubs.acs.org/acscatalysis

Selective Catalytic Olefin Epoxidation with Mn^{II}-Exchanged MOF-5

Amanda W. Stubbs,[†] Luca Braglia,[‡,§] Elisa Borfecchia,[‡] Randall J. Meyer,[∥] Yuriy Román- Leshkov,[⊥] Carlo Lamberti,[‡,§] and Mircea Dincă*[,†]

[†]Department of Chemistry, Massachusetts Institute of Technology, 77 Massachusetts Avenue, Cambridge, Massachusetts 02139, United States

[‡]Department of Chemistry, NIS and CrisDi Interdepartmental Centers, INSTM Reference Center, University of Turin, Via P Giuria 7, I-10125 Turin, Italy

[§]International research center "Smart Materials", Southern Federal University, 5 Zorge Street, Rostov-on-Don 344090, Russia

[∥]Corporate Strategic Research, ExxonMobil Research and Engineering, 1545 Route 22, Annandale, New Jersey 08801, United States

[⊥]Department of Chemical Engineering, Massachusetts Institute of Technology, 77 Massachusetts Avenue, Cambridge, Massachusetts 02139, United States

Supporting Information

ABSTRACT: Partial substitution of Zn^{II} by Mn^{II} in Zn_4O-(terephthalate)$_3$ (MOF-5) leads to a distorted all-oxygen ligand field supporting a single Mn^{II} site, whose structure was confirmed by Mn K-edge X-ray absorption spectroscopy. The Mn^{II} ion at the MOF-5 node engages in redox chemistry with a variety of oxidants. With ^{t}BuSO$_2$PhIO, it produces a putative Mn^{IV}-oxo intermediate, which upon further reaction with adventitious hydrogen is trapped as a Mn^{III}−OH species. Most intriguingly, the intermediacy of the high-spin Mn^{IV}−oxo species is likely responsible for catalytic activity of the Mn^{II}-MOF-5 precatalyst, which in the presence of ^{t}BuSO$_2$PhIO catalyzes oxygen atom transfer reactivity to form epoxides from cyclic alkenes with >99% selectivity. These results demonstrate that MOF secondary building units serve as competent platforms for accessing terminal high-valent metal−oxo species that consequently engage in catalytic oxygen atom transfer chemistry owing to the relatively weak ligand fields provided by the SBU.

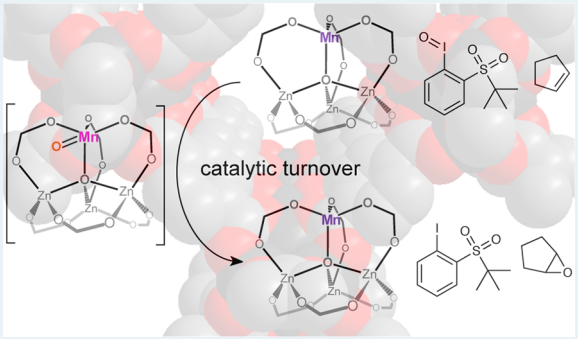

KEYWORDS: *alkene epoxidation, metal−organic framework, manganese(IV)−oxo, manganese(III)−hydroxo, tert-butylsulfonyl-2-iodosylbenzene, oxidation, heterogeneous catalysis*

INTRODUCTION

In catalysis, metal−organic frameworks (MOFs) combine the benefits of heterogeneous catalysts, such as ease of recovery and product separation, with those of homogeneous catalysts, most critically steric and electronic tunability.[1−4] Furthermore, metal ions comprising the MOF secondary building units (SBUs) exhibit biomimetic features that are desirable but difficult to replicate in homogeneous systems. These include high-spin electronic configurations, determined by the weak ligand fields of traditional MOF ligands (e.g., carboxylates, azolates), site isolation, and multiple open coordination sites. In combination with postsynthetic metal exchange, which can be utilized to install non-native metal ions within a large variety of MOFs,[5] the unique properties of SBUs can be harnessed to explore fundamentally new coordination chemistry and catalysis. The versatility of SBU-based chemistry and the particular importance of site isolation conferred by MOFs was highlighted by us and others in the characterization of highly reactive species, such as the first example of a ferric hyponitrite in Fe-exchanged Zn_4O(terephthalate)$_3$ (MOF-5),[6] and the development of industrially relevant catalysts, such as the heterogenization of an ion-pair molecular catalyst for the selective carbonylation of epoxides[7] and an ethylene dimerization catalyst that exhibits an unprecedented combination of activity and selectivity for 1-butene.[8]

Encouraged by these results, we sought to explore the potential utility of cation exchange and SBU chemistry in reactions that typically suffer from poor selectivity due to uncontrolled radical processes. A vast set of reactions fits this criterion, but few are as relevant industrially as hydrocarbon oxidations. Although hydrocarbon oxidations are practiced on a massive industrial scale, they typically require the intermediacy of high-valent metal−oxygen species whose reactivity is difficult to control.[9] Selectivity in these processes is further affected by both kinetics and thermodynamics: C−H bonds in oxidized (oxygenated) products are often more reactive than those of

Received: August 29, 2017
Revised: November 29, 2017
Published: November 30, 2017

DOI: 10.1021/acscatal.7b02946
ACS Catal. 2018, 8, 596−601

alkanes or olefins, which leads to undesired oxidation of the products and eventual formation of CO_2, the thermodynamic sink.[10] This is most famously exemplified by the selective oxidation of methane to methanol, a natural process that is not practiced on an industrial scale because there are no known catalysts that can selectively react with the C−H bonds in methane but not those in methanol with sufficient activity.[11] Other targets of industrial interest abound and include aromatic oxidations, benzylic oxidations,[12] and olefin epoxidations.[13] Indeed, oxygenates represent some of the most versatile commodity chemicals,[9,14] justifying the continued interest in the discovery of new selective oxidation catalysts from both a fundamental and an applied perspective.[15] Here, we show that Mn^{II} ions supported within the unusually weak field zinc−carboxylate SBUs of MOF-5 (Figure 1) engage in oxidative reactivity and serve as selective catalysts for the epoxidation of cyclopentene, through the likely intermediacy of a high-spin Mn^{IV}−oxo complex.

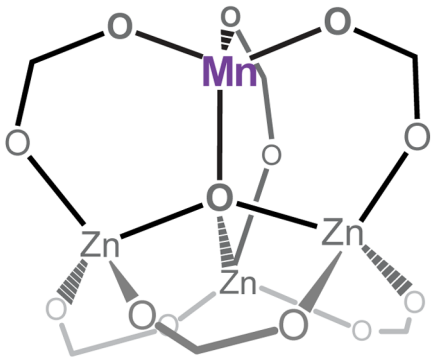

Figure 1. $MnZn_3O(terephthalate)_3$ cluster.

We selected Mn-MOF-5 as a potential precatalyst because it offers a unique coordination environment around redox-active Mn ions. Examples of mononuclear Mn^{II} complexes that demonstrate oxygen atom transfer reactivity frequently invoke Mn^{IV}−oxo as an intermediate; the molecular examples of isolated Mn^{IV}−oxos feature ligand fields that are exclusively or largely based on nitrogen donor ligands.[16−19] Mononuclear complexes with predominantly oxygen ligand fields are scarce, yet some manganese-containing enzymes have carboxylate ligands.[20,21] Thus, studying Mn in the MOF-5 ligand field should provide valuable information about the effects of such a ligand environment as well as potentially provide insight into the underpinnings of Mn-based enzymes. Indeed, given that most known examples of isolated Mn^{IV}−oxos are in an all-nitrogen ligand environment, we surmised that an even more reactive species could be generated in an all-oxygen ligand environment since the carboxylates comprising the SBU of MOF-5 are weaker donors. We also reasoned that the site-isolated environment provided by the framework could enhance the lifetime of the high-valence intermediate by preventing dimerization or other deactivating reactions.[6] With our approach, we thus targeted a system that would exhibit increased reactivity by providing less electronic stability to the presumed Mn^{IV}−oxo intermediate.

RESULTS AND DISCUSSION

Installation of Mn^{II} within the SBU of MOF-5 followed a previously reported procedure[22] with slight modifications aimed at improving the crystallinity and surface area of the Mn^{II}-exchanged MOF-5 (heretofore referred to as Mn^{II}-MOF-5). In particular, because Mn^{II} exchanges very rapidly into MOF-5, lowering the temperature of the exchange to −35 °C and reducing the concentration of Mn^{II} in the exchanging solution to the molar ratio Mn^{II}:$Zn_4O(BDC)_3$ = 4:1 yielded high-quality material with a powder X-ray diffraction (PXRD) pattern which matched that of original MOF-5 (Figure S1 in the Supporting Information). The Brunauer−Emmett−Teller (BET) apparent surface area of this material, measured by an N_2 adsorption isotherm at 77 K, was 3100 m^2/g (Figure S2 in the Supporting Information), a notable improvement over the previously reported value of 2400−2700 m^2/g[22] and in line with that reported for the original MOF-5.[23] Inductively coupled plasma−mass spectrometry (ICP-MS) of Mn^{II}-MOF-5 samples prepared by this procedure consistently gave Mn:Zn ratios of approximately 1:15, corresponding to one Mn^{II} ion in every four SBUs and a formula unit of $Mn_{0.25}Zn_{3.75}(BDC)_3$ (Mn^{II}_{high}-MOF-5). We deemed this relatively low loading of Mn^{II} desirable because reactive species at MOF SBUs can be a structural liability for the integrity of the entire MOF.

The electronic structure of the Mn^{II} ions in Mn^{II}-MOF-5 was probed by continuous-wave electron paramagnetic resonance (EPR) spectroscopy. X-band spectra of suspensions of Mn^{II}_{high}-MOF-5 in tetrahydrofuran (THF) frozen at 77 K exhibit a single, very broad signal, indicative of fast spin−spin relaxation pathways likely stemming from the close proximity of Mn^{II} ions. To eliminate spin−spin interactions, we sought to separate the Mn^{II} ions within the MOF-5 lattice even further and found that direct synthesis is more effective than postsynthetic cation exchange in forming more magnetically dilute Mn^{II}-MOF-5. Thus, heating a solution of $Mn(NO_3)_2\cdot 6H_2O$ with a large excess of $Zn(NO_3)_2\cdot 6H_2O$ and terephthalic acid yielded a crystalline and porous Mn^{II}-MOF-5 sample containing only 1 Mn atom for every 155 Zn atoms, corresponding to the formula unit $Mn_{0.026}Zn_{3.974}O(BDC)_3$ (Mn^{II}_{low}-MOF-5). X-band EPR spectra of this magnetically dilute material confirmed the essentially complete elimination of spin−spin interactions between Mn^{II} sites and exhibited an isotropic signal with the six lines of hyperfine coupling characteristic of high-spin $^{55}Mn^{II}$, at g = 2.021 and with a = 88 G (Figure 2).[24,25]

With evidence in hand of a Mn^{II} ion isolated in a relatively weak ligand field, Mn^{II}-MOF-5 was subjected to a variety of common oxidants to probe the redox reactivity of the Mn^{II} center. Although Mn^{II}-MOF-5 shows no reactivity in the

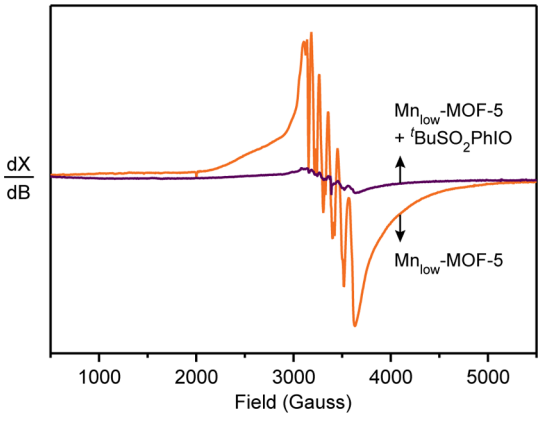

Figure 2. EPR of Mn-MOF-5 collected at 77 K in THF.

DOI: 10.1021/acscatal.7b02946
ACS Catal. 2018, 8, 596−601

presence of O_2 between −77 and 150 °C, it reacts readily with a variety of oxygen atom transfer (OAT) reagents. Thus, colorless crystals of Mn^{II}_{high}-MOF-5 exposed to a colorless solution of pyridine *N*-oxide (PyNO) undergo a vivid color change to lime green, quantified by diffuse-reflectance UV−vis (DRUV−vis) spectroscopy as a new absorbance at 400 nm (Figure 3). However, the EPR signal from Mn sites upon

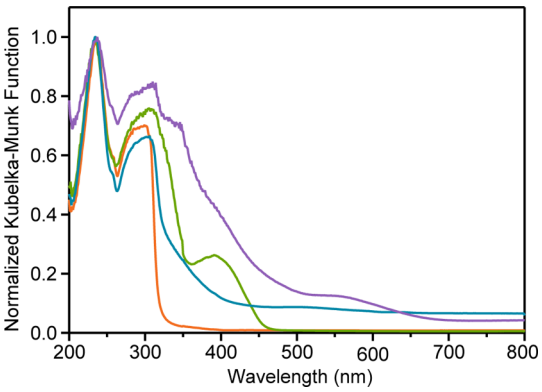

Figure 3. DRUV−vis of Mn-MOF-5 crystals after soaking in dichloromethane (DCM) (orange) and DCM solutions of PyNO (green), MesCNO (blue), and ^{t}BuSO$_2$PhIO (purple).

reaction with PyNO, investigated using a Mn^{II}_{low}-MOF-5 sample to avoid spin−spin relaxation, was identical with that of unoxidized Mn^{II}-MOF-5 regardless of the reaction temperature. This suggests that the formal oxidation state of Mn remains 2+ upon reaction with PyNO and that the observed color change is due to a ligand-to-metal charge transfer band rather than a d−d transition, as may be expected from Mn^{III} or Mn^{IV}. A variety of other OAT reagents of varying N−O bond strengths, including mesityl nitrile *N*-oxide (MesCNO, N−O bond dissociation energy (BDE_{N-O}) = 53 kcal/mol) and N_2O (BDE_{N-O} = 34 kcal/mol)[26] were similarly incapable of oxidizing the Mn atoms in Mn^{II}-MOF-5 and gave either no visible reactions or colored products with EPR signals characteristic of Mn^{II}.

Although N_2O has a very low BDE_{N-O} value, we reasoned that its lack of redox activity toward Mn^{II}-MOF-5 is kinetic, rather than thermodynamic,[27] and that other reagents with readily transferable O atoms may yet be able to oxidize Mn^{II}-MOF-5. In this sense, one reagent that has been reported to yield isolable Mn^{IV}−oxo complexes is iodosobenzene and its more soluble version *tert*-butylsulfonyl-2-iodosylbenzene (^{t}BuSO$_2$PhIO).[19,28] Upon exposure to a yellow solution of the latter, crystals of Mn-MOF-5 turn deep purple over 12 h. This color is associated with a new absorption at 550 nm (Figure 3) that was not observed with the other OAT reagents. Most significantly, the EPR spectrum of Mn^{II}_{low}-MOF-5 crystals treated with ^{t}BuSO$_2$PhIO revealed a significantly diminished Mn^{II} signal (Figure 2), with no overlap from other paramagnetic species. This suggested that the majority of Mn^{II} sites have been oxidized and transformed into an EPR-silent species, likely Mn^{III}. Although we expected that ^{t}BuSO$_2$PhIO would produce a Mn^{IV}−oxo, it is not unusual for reactive metal−oxo species to abstract hydrogen atoms from solvents, including DCM, as used here.[29] Indeed, when Mn^{II}_{high}-MOF-5 was treated with ^{t}BuSO$_2$PhIO in deuterated chloroform ($CDCl_3$) in the presence of cyclohexadiene, an excellent H atom donor, quantitative formation of benzene was observed, suggesting the intermediacy of a Mn^{IV}−oxo and likely formation of Mn^{III}−OH. Complete exclusion of H atom donors from the reaction mixture to ideally isolate this putative Mn^{IV}−oxo was unfortunately not possible because the solubility of ^{t}BuSO$_2$PhIO is limited to DCM and $CHCl_3$. The oxidation state and the structure of the Mn^{III} site obtained from oxidation of Mn^{II}-MOF-5 with ^{t}BuSO$_2$PhIO was further probed by Mn K-edge X-ray absorption spectroscopy (XAS). X-ray absorption near-edge spectroscopy (XANES) revealed that Mn^{II}-MOF-5 presents the same features and edge position as $MnCl_2$, our reference for Mn^{II} (Figure 4a). In contrast, the absorption edge for the material obtained by oxidation of Mn^{II}_{high}-MOF-5 with ^{t}BuSO$_2$PhIO, purportedly Mn^{III}(OH)-MOF-5, shifts to higher energy and approaches that of Mn_2O_3, our reference for Mn^{III}. Additionally, its white line decreases, also in line with that of Mn_2O_3 (Figure 4b). Edge shifts by $\Delta E \approx 3$ eV accompanied by a significant decrease and broadening of the white line are characteristic for changes in oxidation state from Mn^{II} to Mn^{III}.[30−33] Although the edge position in the XANES spectrum of Mn^{III}(OH)-MOF-5 is closer to that of Mn^{III} in Mn_2O_3 than to those of MnO and $MnCl_2$, it is clearly intermediate between Mn^{II} and Mn^{III}. This implies that Mn^{III}(OH)-MOF-5 contains a dominant fraction of Mn^{III} together with a residual amount of Mn^{II}, in further agreement with the EPR studies (vide supra).

Structural insight into the local environment of the Mn sites in Mn^{II}-MOF-5 came from analysis of the extended X-ray

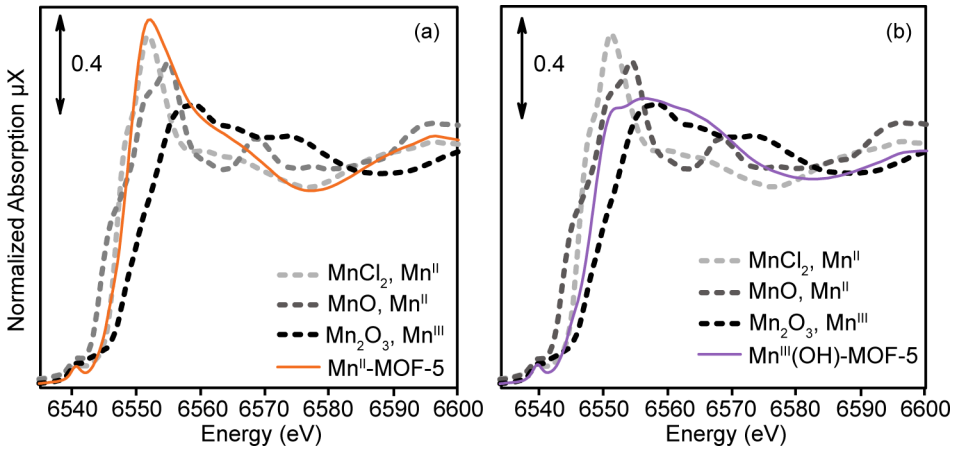

Figure 4. Mn K-edge XANES spectra of Mn^{II}-MOF-5 (a) and Mn^{III}(OH)-MOF-5 (b) in comparison with reference compounds.

DOI: 10.1021/acscatal.7b02946
ACS Catal. 2018, 8, 596−601

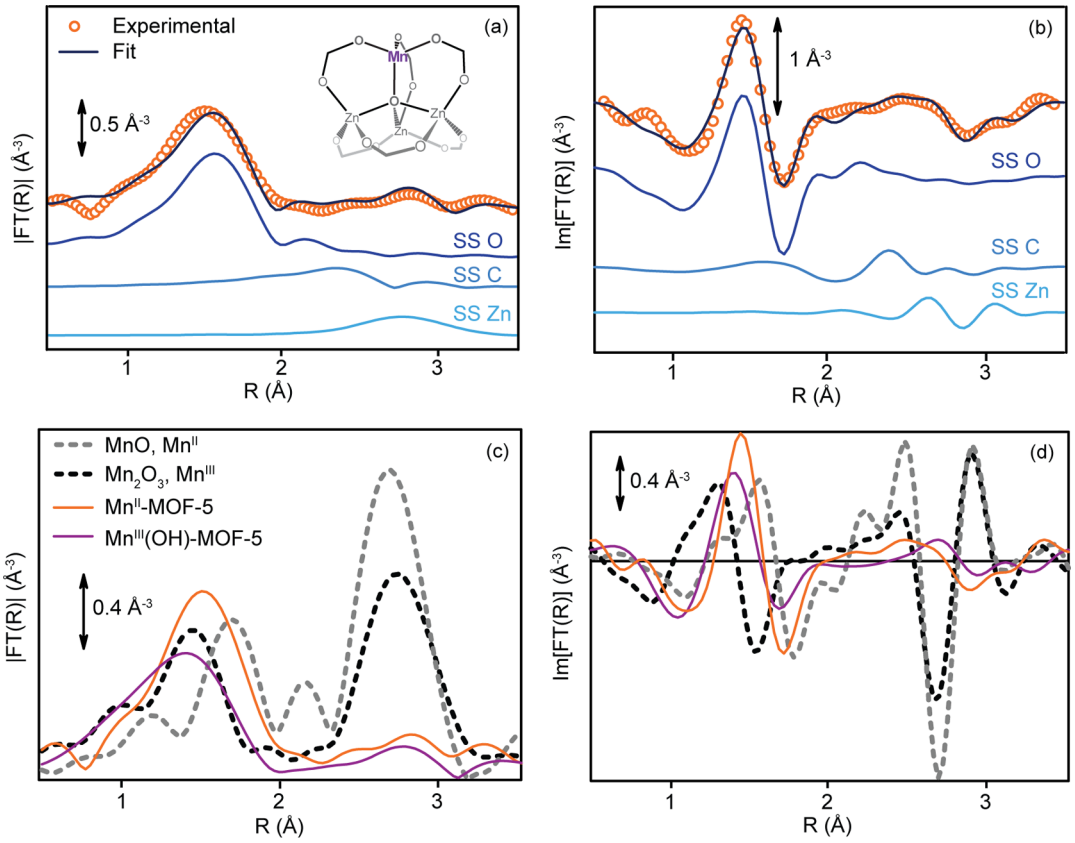

Figure 5. Modulus (a) and imaginary part (b) of the experimental and best-fit k^2-weighted, phase-uncorrected FT of the EXAFS spectra for Mn^{II}-MOF-5. Single scattering (SS) contributions involving the O, C, and Zn atomic neighbors are also reported. Modulus (c) and imaginary part (d) of the phase-uncorrected FT of experimental EXAFS spectra for Mn^{III}(OH)-MOF-5 in comparison with the references and experimental spectrum of Mn^{II}-MOF-5.

absorption fine structure (EXAFS) data. To model these data, we employed a DFT-optimized SBU fragment, where the absorbing Mn atom is surrounded by four O atoms in the first coordination shell and three C and three Zn atoms in the second coordination shell (inset Figure 5a). This structure provides a good EXAFS fit with the experimental data (Figure 5a,b and Table S1 in the Supporting Information), revealing the mean Mn−O bond distance R_{Mn-O} = 2.07 ± 0.01 Å and second-shell mean distances $R_{Mn\cdots C}$ = 3.00 ± 0.04 Å and $R_{Mn\cdots Zn}$ = 3.23 ± 0.03 Å. Notably, the optimized Debye−Waller factor for the Mn···Zn contribution, σ^2_{Zn} = 0.015 Å^2 (Table S1), is too high to have a pure vibrational origin. Indeed, the corresponding Debye−Waller factor obtained in fitting the Zn···Zn contribution in a spectrum of pure Zn-MOF-5, collected at 25 °C, was previously optimized to 0.009 Å^2.[34] This discrepancy is a clear indication of structural local disorder in Mn^{II}-MOF-5, with the consequent appearance of three slightly different Mn···Zn distances. These cannot be resolved in the EXAFS analysis and likely account for the amplitude decrease in the EXAFS second-shell signal and the corresponding increase in the Debye−Waller parameter.

Surprisingly, although a qualitative analysis of the Fourier transform (FT) of the EXAFS spectrum of Mn^{III}(OH)-MOF-5 shows a decrease in the apparent Mn−O coordination distance in the first shell relative to that observed in Mn^{II}-MOF-5, the data also show significantly damped intensity despite the expected increase in coordination number from 4 to 5 (Figure 5c,d). We attribute this counterintuitive observation to the small quantity of Mn^{II} left over after treatment of Mn^{II}-MOF-5 with ^{t}BuSO$_2$PhIO. Because the Mn−O distances at Mn^{III} and leftover Mn^{II} sites in Mn^{III}(OH)-MOF-5 differ, scattering from the Mn^{II} site is in antiphase with that from the Mn^{III} site, which can account for the observed first-shell signal damping in this material relative to the pure Mn^{II}-MOF-5 sample.

With experimental evidence that ^{t}BuSO$_2$PhIO is able to generate, at least transiently, a high-valent, all-oxygen Mn^{IV}−oxo moiety capable of further reactivity, we sought to find substrates where O atom transfer reactivity, rather than H atom abstraction chemistry, would be observed. We found that the combination of Mn^{II}_{high}-MOF-5 and ^{t}BuSO$_2$PhIO effects the selective oxidation of cyclopentene to cyclopentene oxide catalytically in $CDCl_3$. Reaction conditions were optimized to yield a maximum of seven turnovers per Mn site; this was achieved with 300 equiv of substrate (relative to moles of Mn present), minimal solvent, and 50 equiv of ^{t}BuSO$_2$PhIO added incrementally. Through the optimization process a linear correlation between moles of substrate produced and moles of oxidant added became evident (Figure 6). However, the trend plateaued at the observed maximum of 7 equiv of cyclopentene oxide produced. PXRD of the Mn-MOF-5 after this maximum output reaction revealed the beginning of decomposition of the framework, with a loss of crystallinity and splitting of low-angle peaks (Figure S1 in the Supporting Information). Reactions in which MOF-5 was substituted for Mn^{II}_{high}-MOF-5 resulted in no oxidation of the substrate, indicating that merely Lewis acid catalysis at the Zn atoms in the framework is not sufficient to produce the OAT reactivity observed with Mn^{II}_{high}-MOF-5.

DOI: 10.1021/acscatal.7b02946
ACS Catal. 2018, 8, 596−601

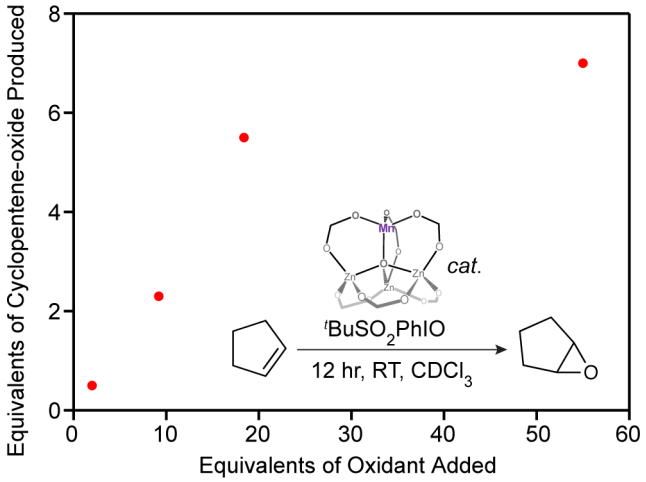

Figure 6. Catalytic cyclopentene oxidation by Mn-MOF-5 and $^{t}BuSO_2PhIO$, with conversion plotted as a function of equivalents of oxidant added. The 55 equiv of oxidant that was introduced for the final data point was added in portions over the course of 7 days to prevent disproportionation of the oxidant as a result of slow consumption.

Knowing that a likely competing reaction to epoxidation is H atom abstraction from solvent, we tested whether Mn^{III}(OH)-MOF-5 serves as a competent precatalyst for OAT to cyclopentene. Exposure of Mn^{III}(OH)-MOF-5 to additional oxidant and cyclopentene produced more than 1 equiv of cyclopentene oxide per Mn, suggesting that Mn^{III}(OH)-MOF-5 indeed is a viable precatalyst for the epoxidation of cyclopentene. Reactions in which Mn^{III}(OH)-MOF-5 was exposed to cyclopentene in the absence of additional oxidant resulted in no OAT reactivity, eliminating it as the active catalytic species. Mn ions leached from the framework were also ruled out as the responsible species for OAT reactivity by a hot filtration experiment as well as experiments where Mn salts such as $MnCl_2$, $MnCl_2$ with terephthalic acid, MnO_2, and Mn_2O_3 were substituted for Mn^{II}_{high}-MOF-5 (see the Supporting Information).

The Mn^{II}_{high}-MOF-5 and $^{t}BuSO_2PhIO$ system serves as very selective epoxidation catalyst for other cyclic alkenes, such as cyclohexene and norbornene, which are oxidized to the corresponding epoxides with selectivities greater than 99%. However, the relative reactivity with each substrate correlates directly with the amount of ring strain (Table 1), and the system is not effective in the oxidation of noncyclic olefins to epoxides or any other oxidized species, or in the oxidation of other hydrocarbons such as cumene and cyclohexane. Thus, ring strain is a necessary driving force for epoxidations by this system, and hydroxylation is not a viable reaction pathway. The lack of reactivity toward hydroxylation is perhaps best explained by the fact that the rebound mechanism often invoked in C−H bond hydroxylation is not possible here due to the high stability of the Mn^{III}−OH intermediate. Other metal ions may provide less stable hydroxyl species, and thus hydroxylation reactivity, a possibility that we are currently exploring. Additionally, we note that epoxidation reactivity requires an unobstructed approach of the double bond to the Mn site. Indeed, we found that, despite the considerable ring strain, 1-methylcyclopentene displays no reactivity with our system. Finally, reactivity takes place primarily within the pores of the MOF, not just on the surface of crystals, as demonstrated by size exclusion experiments with larger cyclic olefins. Thus, cyclododecene, despite a relatively high ring strain value,[35] undergoes less than one turnover when it is subjected to reaction conditions. We surmise that the low reactivity of this molecule is due to its size (7.2 Å at its widest point, not including the solvation sphere), which does not allow it to easily penetrate the approximately 10 Å pores of MOF-5, an observation that is consistent with the use of this substrate in systems with similar pore sizes.[36]

Table 1. Correlation of Substrate Reactivity on Ring Strain Energy

substrate	no. of turnovers per Mn[a]	ring strain energy (kcal/mol)[37]
norbornene	8.80	21.6[37]
cyclopentene	5.52	4.8[37]
1-methylcyclopentene	0	3.9[37]
cyclohexene	1.55	0.3[37]
cyclooctene	3.60	7.0[35]
cyclododecene	0.60	10[35]

[a]Reaction conditions: 10 mg of Mn^{II}_{high}-MOF-5, 600 equiv of substrate, 8 equiv of oxidant, 0.7 mL of $CDCl_3$, 18 h, room temperature.

Fundamentally, the Mn^{II}-MOF-5 system allows the unique opportunity to study the reactivity of a rare terminal Mn^{III}−OH species. Most molecular examples of Mn^{III}−OH species are poor candidates for reactivity studies due to the amount of steric bulk that is necessary to keep such a moiety from dimerizing or forming μ-oxo/-hydroxo bridges.[29,38,39] In turn, when known Mn^{III}−OH species do not require steric protection, they tend to have limited or noncatalytic reactivity.[40,41] As is the case with some of the existing examples, it is reasonable to assume that the formation of Mn^{III}(OH)-MOF-5 proceeds through a Mn^{IV}−oxo intermediate.[29] Although the $Mn^{III/V}$ couple is better known for selective epoxidation reactivity,[42,43] it is not unprecedented for Mn^{II} to generate epoxides in the presence of an oxidant, though not as selectively as we have shown in this work.[44] Importantly, Mn^{IV}−oxo species generated from Mn^{II} precursors can also produce various distributions of alcohols and downstream epoxide oxidation products by introducing small changes in experimental conditions (such as ligand scaffold or protonation of the oxo with HOTf).[45] In our system, the eventual decomposition of Mn^{II}_{high}-MOF-5 over multiple consecutive turnovers further suggests the occurrence of a Mn^{IV}−oxo intermediate. The current reactivity nevertheless suggests that, with small changes, the product distribution may be changed in a fashion mimicking that seen in molecular systems.

CONCLUSION

The foregoing results demonstrate that Mn^{II}-MOF-5 is competent for oxygen atom transfer reactivity in a catalytic fashion. Although the relative instability of this system under sustained catalytic conditions likely prevents its use in industrial applications, the demonstrated reactivity and proposed intermediate highlight a unique opportunity with MOFs to study species of fundamental interest. Specifically, the observed reactivity and the isolation of a terminal Mn^{III}−OH moiety are consistent with the transient formation of a Mn^{IV}−oxo species. This putative high-valent Mn species acts as a highly selective catalyst for the epoxidation of cyclic olefins, a reactivity that is reproduced with the Mn^{III}−OH species, itself a rare occurrence

DOI: 10.1021/acscatal.7b02946
ACS Catal. 2018, 8, 596−601

in a weak ligand field environment such as that afforded by the nodes of MOF-5.

■ ASSOCIATED CONTENT

Supporting Information

The Supporting Information is available free of charge on the ACS Publications website at DOI: 10.1021/acscatal.7b02946.

Details of experimental procedures and results, PXRD, and nitrogen isotherm data (PDF)

■ AUTHOR INFORMATION

Corresponding Author

*E-mail for M.D.: mdinca@mit.edu.

ORCID

Amanda W. Stubbs: 0000-0002-5539-273X
Randall J. Meyer: 0000-0002-0679-0029
Yuriy Román- Leshkov: 0000-0002-0025-4233
Carlo Lamberti: 0000-0001-8004-2312
Mircea Dincă: 0000-0002-1262-1264

Notes

The authors declare no competing financial interest.

■ ACKNOWLEDGMENTS

This research was supported by ExxonMobil Corporate Strategic Research through the MIT Energy Initiative. A.W.S. gratefully acknowledges the National Science Foundation Graduate Research Fellowship program for financial support under Grant No. 1122374. Fundamental studies of cation exchange are supported through an NSF Career grant to M.D. (DMR-1452612). We thank Dr. G. Agostini for assistance with the XAS data collection at ESRF BM23 and Dr. H. Müller for his support in the ESRF chemistry laboratory. Kirill A. Lomachenko and Andrea Melloni are acknowledged for their support during the XAS data collection and for fruitful discussions on the XAS data analysis. C.L. and L.B. acknowledge the Mega-grant of the Russian Federation Government (14.Y26.31.0001).

■ REFERENCES

(1) Chughtai, A. H.; Ahmad, N.; Younus, H. A.; Laypkov, A.; Verpoort, F. *Chem. Soc. Rev.* **2015**, *44*, 6804−6849.
(2) Farrusseng, D.; Aguado, S.; Pinel, C. *Angew. Chem., Int. Ed.* **2009**, *48*, 7502−7513.
(3) Gascon, J.; Corma, A.; Kapteijn, F.; Llabrés i Xamena, F. X. *ACS Catal.* **2014**, *4*, 361−378.
(4) Furukawa, H.; Cordova, K. E.; O'Keeffe, M.; Yaghi, O. M. *Science* **2013**, *341*, 1230444−1230444.
(5) Brozek, C. K.; Dincă, M. *Chem. Soc. Rev.* **2014**, *43*, 5456−5467.
(6) Brozek, C. K.; Miller, J. T.; Stoian, S. A.; Dincă, M. *J. Am. Chem. Soc.* **2015**, *137*, 7495−7501.
(7) Park, H. D.; Dincă, M.; Román-Leshkov, Y. *ACS Cent. Sci.* **2017**, *3*, 444−448.
(8) Metzger, E. D.; Brozek, C. K.; Comito, R. J.; Dincă, M. *ACS Cent. Sci.* **2016**, *2*, 148−153.
(9) Centi, G.; Cavani, F.; Trifirò, F. Trends and Outlook in Selective Oxidation: An Introduction. In *Selective Oxidation by Heterogeneous Catalysis*, 1st ed.; Springer US, :New York, 2001; pp 1−24.
(10) Labinger, J. A.; Bercaw, J. E. *Nature* **2002**, *417*, 507−514.
(11) Ravi, M.; Ranocchiari, M.; van Bokhoven, J. A. *Angew. Chem., Int. Ed.* **2017**, *56*, 2−22.
(12) Centi, G.; Cavani, F.; Trifirò, F. New Concepts and New Strategies in Selective Oxidation. In *Selective Oxidation by Heterogeneous Catalysis*, 1st ed.; Springer US: New York, 2001; pp 325−362.
(13) Whittall, J. In *Regio- and Stereo- Controlled Oxidations and Reductions*; Roberts, S. M., Whittall, J., Eds.; Wiley: Chichester, U.K., 2007; Vol. *5*, pp 1−33.
(14) Werpy, T.; Petersen, G. *Top Value Added Chemicals from Biomass Vol. I — Results of Screening for Potential Candidates from Sugars and Synthesis Gas*; US Department of Energy: Washington, DC, USA, 2004; DOE/GO-102004-1992, p 10.
(15) Kuwahara, Y.; Yoshimura, Y.; Yamashita, H. *Dalt. Trans.* **2017**, *46*, 8415−8421.
(16) Barman, P.; Vardhaman, A. K.; Martin, B.; Wörner, S. J.; Sastri, C. V.; Comba, P. *Angew. Chem., Int. Ed.* **2015**, *54*, 2095−2099.
(17) Parsell, T. H.; Behan, R. K.; Green, M. T.; Hendrich, M. P.; Borovik, A. S. *J. Am. Chem. Soc.* **2006**, *128*, 8728−8729.
(18) Wu, X.; Seo, M. S.; Davis, K. M.; Lee, Y.-M.; Chen, J.; Cho, K.-B.; Pushkar, Y. N.; Nam, W. *J. Am. Chem. Soc.* **2011**, *133*, 20088−20091.
(19) Yoon, J.; Seo, M. S.; Kim, Y.; Kim, S. J.; Yoon, S.; Jang, H. G.; Nam, W. *Bull. Korean Chem. Soc.* **2009**, *30*, 679−682.
(20) Whittaker, M. M.; Barynin, V. V.; Antonyuk, S. V.; Whittaker, J. W. *Biochemistry* **1999**, *38*, 9126−9136.
(21) Ferreira, K. N. *Science* **2004**, *303*, 1831−1838.
(22) Brozek, C. K.; Dincă, M. *J. Am. Chem. Soc.* **2013**, *135*, 12886−12891.
(23) Kaye, S. S.; Dailly, A.; Yaghi, O. M.; Long, J. R. *J. Am. Chem. Soc.* **2007**, *129*, 14176−14177.
(24) Matzapetakis, M.; Karligiano, N.; Bino, A.; Dakanali, M.; Raptopoulou, C. P.; Tangoulis, V.; Terzis, A.; Giapintzakis, J.; Salifoglou, A. *Inorg. Chem.* **2000**, *39*, 4044−4051.
(25) Reed, G. H.; Cohn, M. *J. Biol. Chem.* **1973**, *248*, 6436−6442.
(26) Holm, R. H.; Donahue, J. P. *Polyhedron* **1993**, *12*, 571−589.
(27) Severin, K. *Chem. Soc. Rev.* **2015**, *44*, 6375−6386.
(28) Yoon, H.; Morimoto, Y.; Lee, Y.-M.; Nam, W.; Fukuzumi, S. *Chem. Commun.* **2012**, *48*, 11187−11189.
(29) Shirin, Z.; Young, V. G.; Borovik, A. S. *Chem. Commun.* **1997**, *36*, 1967−1968.
(30) Fernández, G.; Corbella, M.; Alfonso, M.; Stoeckli-Evans, H.; Castro, I. *Inorg. Chem.* **2004**, *43*, 6684−6698.
(31) Stueben, B. L.; Cantrelle, B.; Sneddon, J.; Beck, J. N. *Microchem. J.* **2004**, *76*, 113−120.
(32) Manceau, A.; Marcus, M. A.; Grangeon, S. *Am. Mineral.* **2012**, *97*, 816−827.
(33) Xu, L.; Liu, W.; Li, X.; Rashid, S.; Shen, C.; Wen, Y. *RSC Adv.* **2015**, *5*, 12248−12256.
(34) Hafizovic, J.; Bjørgen, M.; Olsbye, U.; Dietzel, P. D. C.; Bordiga, S.; Prestipino, C.; Lamberti, C.; Lillerud, K. P. *J. Am. Chem. Soc.* **2007**, *129*, 3612−3620.
(35) Lerum, M. F. Z.; Chen, W. *Langmuir* **2011**, *27*, 5403−5409.
(36) Moliner, M.; Serna, P.; Cantin, A.; Sastre, G.; Diaz-Cabanas, M. J.; Corma, A. *J. Phys. Chem. C* **2008**, *112*, 19547−19554.
(37) Khoury, P. R.; Goddard, J. D.; Tam, W. *Tetrahedron* **2004**, *60*, 8103−8112.
(38) Shook, R. L.; Peterson, S. M.; Greaves, J.; Moore, C.; Rheingold, A. L.; Borovik, A. S. *J. Am. Chem. Soc.* **2011**, *133*, 5810−5817.
(39) Shirin, Z.; Hammes, B. S.; Young, V. G.; Borovik, A. S. *J. Am. Chem. Soc.* **2000**, *122*, 1836−1837.
(40) Goldsmith, C. R.; Cole, A. P.; Stack, T. D. P. *J. Am. Chem. Soc.* **2005**, *127*, 9904.
(41) Eichhorn, D. M.; Armstrong, W. H. *J. Chem. Soc., Chem. Commun.* **1992**, *20*, 85−87.
(42) Guo, M.; Dong, H.; Li, J.; Cheng, B.; Huang, Y.; Feng, Y.; Lei, A. *Nat. Commun.* **2012**, *3*, 1190.
(43) Collman, J. P.; Zeng, L.; Wang, H. J. H.; Lei, A.; Brauman, J. I. *Eur. J. Org. Chem.* **2006**, *2006*, 2707−2714.
(44) Lymperopoulou, S.; Papastergiou, M.; Louloudi, M.; Raptopoulou, C. P.; Psycharis, V.; Milios, C. J.; Plakatouras, J. C. *Eur. J. Inorg. Chem.* **2014**, *2014*, 3638−3644.
(45) Kim, S.; Cho, K.-B.; Lee, Y.-M.; Chen, J.; Fukuzumi, S.; Nam, W. *J. Am. Chem. Soc.* **2016**, *138*, 10654−10663.

DOI: 10.1021/acscatal.7b02946
ACS Catal. 2018, 8, 596−601